Modelling of short runout propagation landslides and debris flows

Mila E. Sanchez , Manuel Pastor and Manuel G. Romana

This paper proposes an extension of methods used to predict the propagation of landslides having a long runout to smaller landslides with much shorter propagation distances. The method is based on: (1) a depth-integrated mathematical model including the coupling between the soil skeleton and the pore fluids, (2) suitable rheological models describing the relation between the stress and the rate of deformation tensors for fluidised soils and (3) a meshless numerical method, Smooth Particle Hydrodynamics, which separates the computational mesh (or set of computational nodes) from the mesh describing the terrain topography, which is of structured type – thus accelerating search operations. The proposed model is validated using two examples for which there are analytical solutions, and then it is applied to two short runout landslides which happened in Hong Kong in 1995, for which there is available information.

Keywords: fast landslides; SPH; fluidised geomaterials; debris flows; short runout; propagation

1. Introduction

Landslides are natural disasters that cause large economic damage and losses of human lives. It is important, therefore, to understand their triggering mechanisms and to predict their effects, quantifying the runout distance, velocity and depth. Consequently, the use of quantitative models for both initiation and propagation phases is fundamental for engineers, geologists and other scientists dealing with the effects of landslides.

There are many simplified methods in both cases for providing quantitative results. Concerning the determination of the triggering mechanisms – and the conditions under which failure occurs – we can find in the early work of Coulomb (1773) the seed of what we do today. There are simplified methods such as (1) the slip line, (2) limit theorems for plastic collapse and (3) limit equilibrium. All of them provide information on failure loads and mechanisms (Pastor et al. 2010). It is important to notice that in those cases where failure is diffuse, approximated methods are not accurate, as they are based on two main assumptions which are not valid here: (1) the stress state lies on the Mohr Coulomb surface and (2) failure takes place along well-defined surface.

Alternatively, methods based on the use of mathematical models accounting for coupling between soil skeleton and pore fluids, constitutive models and numerical discretisation techniques such as finite elements provide accurate results for both localised and diffuse failure (Zienkiewicz and Taylor 2000).

Concerning propagation, there are cases where the mobility is large, usually associated to pore pressures generated during the triggering of the landslide, while in others the runout is much smaller. Different models have been developed to simulate it (Hutchinson 1986; Hutter and Koch 1991; Savage and Hutter 1991; Laigle and Coussot 1997; Iverson and Denlinger 2001; Pastor et al. 2002, 2004a, 2009; McDougall and Hungr 2004; Poisel and Preh 2004; Quecedo et al. 2004; D'Ambrosio et al. 2007; Iovine and Mangraviti 2009), and most of them are carried out in the framework of continuum mechanics, considering the avalanching mass as a fluid. In some recent works, coupling between the fluidised solid grains and the pore fluid has been taken into account (Hutchinson 1986; Iverson and Denlinger 2001; Pastor et al. 2002, 2004a). A simple approach considers that pore pressure dissipation takes place only in the vertical direction, causing a change in the basal pore pressure.

Many flow-like catastrophic landslides have small average depths in comparison with their length or width. Then, a possible simplification is integrating its equations along the vertical axis. The resulting 2D depth-integrated model presents an excellent combination of accuracy and simplicity, providing important information such as velocity of propagation,

time to reach a particular place, depth of the flow at a certain location, etc. Depth-integrated models have been frequently used in the past to model flow-like landslides. It is worth mentioning the pioneering work of Hutter and Koch (1991), and those of Laigle and Coussot (1997), Pastor et al. (2002), Quecedo et al. (2004) and McDougall and Hungr (2004).

Once the needed initial and boundary conditions are provided, the spatial and temporal integration of the system of differential equations can be done with the aid of numerical methods. Most of them are based on grids, either structured (finite differences) or unstructured (finite elements and volumes). An interesting and powerful alternative to these is provided by a new group of 'meshless' numerical methods that have been developed in the past decades.

Smooth Particle Hydrodynamics (SPH) is a meshless method introduced independently by Lucy (1977) and Gingold and Monaghan (1977), and firstly applied to astrophysical modelling, a domain where SPH presents important advantages over other methods (Monaghan and Lattanzio 1985). SPH is well suited for hydrodynamics, and researchers have applied it to a variety of problems, has also been applied to model the propagation of catastrophic landslides (McDougall and Hungr 2004; Bonet and Rodríguez 2005); however, the analysis did not incorporate the hydro-mechanical coupling between the solid skeleton and the pore fluid.

The SPH method presents the advantage, when dealing with large domains over which the landslide propagates, of using two systems of storing information: (1) a structured mesh for topographical data (height, slope and curvature) and (2) a computational mesh consisting of SPH nodes. In addition to be a Lagrangian method which avoids problems associated to Eulerian formulations, its computational cost is much smaller.

In this paper, an SPH depth-integrated model with coupling between the solid and the fluid phases is proposed to simulate the propagation stage. This model has already been tested successfully in various real phenomena with large runout (Pastor et al. 2009). Therefore, we propose to extend the method to short runout landslides as an economic tool to predict their consequences (runout, velocities and depth of the deposits). We have used a well-documented set of cases provided by Hong Kong Geotechnical Office, who kindly make these data available. These cases occurred after heavy rainfall episodes on August 1995, in the wake of typhoon Helen.

The paper is structured as follows. First, we introduce the mathematical model. A second section is devoted to describe the rheological models used for the benchmarks, followed by a section where we describe the discretisation technique we have used. Finally, we present the selected benchmarks, which include (1) two problems with an analytical solution, (2) a landslide with a small travel distance and (3) a debris flow with a relatively short runout distance.

It is important to note that the proposed method relies on the knowledge of the triggering mechanism and the mobilised mass of soil, which can be obtained by classical finite element analysis, or other suitable alternative techniques. However, classical finite elements cannot represent accurately the whole phenomena – the mobilised mass travelling downhill – unless special and computationally expensive techniques are used. The method proposed here provides a simple and computationally cheap alternative to be used in this part of the analysis.

2. Mathematical model

Soils and rocks are multiphase geomaterials, exhibiting a mechanical behaviour governed by the coupling between the phases. Among the different possibilities, we have chosen an approach close to mixture theory.

The first mathematical model describing the coupling between solid and fluid phases was proposed by Biot (1941, 1955) for linear elastic materials. This work was followed by further developments at Swansea University, where Zienkiewicz and co-workers (1980, 1999) extended the theory to non-linear materials and large deformation problems. It is also worth mentioning the work of Lewis and Schrefler (1998), Coussy (1995) and De Boer (2000).

This theoretical framework began to be applied to model the propagation of landslides two decades ago by Hutchinson (1986), who proposed a sliding consolidation model to predict runout of landslides, and other important works are Iverson and Denlinger (2001), Pastor et al. (2002, 2004a) and Quecedo et al. (2004).

The propagation of a fast landslide is a complex phenomenon involving in many cases a strong coupling between solid and fluid phases, which can have important velocities relative to the solid skeleton. In these cases, we need to use a general model based on mixture theory, where both soil grains and pore fluids may have important relative displacements and velocities.

In many cases, the relative displacements are small, and can be used the first simplified model, the $u-p_w$ algorithm proposed by Zienkiewicz, Chang, and Bettess (1980), Zienkiewicz and Shiomi (1984), Zienkiewicz et al. (1990a,b). Here, it is assumed that the velocity of fluid phases relative to solid skeleton is small, and the equations can be cast in terms of the displacements or velocities of solid skeleton, the

velocities of the pore water relative to the skeleton and the averaged pore pressure of the interstitial fluids. Then under certain assumptions, which were analysed for soil mechanics problems, it is possible to eliminate the Darcy velocity, which results on a model expressed in terms of velocities of the soil skeleton and pore pressures.

In many landslides, their geometry allows to assume that pore pressure dissipation takes place along the normal to the terrain surface, and the velocity and pressure fields can be split into two components: propagation and consolidation. This is referred to as the 'propagation–consolidation' model (Pastor et al. 2004a).

Further simplification leads to depth-integrated models, where it is assumed that the average depth is small in comparison with landslide length and width. The balance of mass and momentum equations is integrated along the depth, and the problem is transformed into a two-dimensional form.

In the following section, we will provide a brief description of the depth-integrated model which has been used to analyse landslides with short runout distances.

2.1. Propagation–consolidation model

The starting point is the $u-p_w$ model, which consists of:

(1) The balance of mass, combined with the balance of linear momentum of the pore fluid, which in the case of saturated soils is:

$$-div(k_w grad(p_w) + div(v_s) + \frac{1}{Q}\frac{Dp_w}{Dt} = 0 \text{ with } \frac{1}{Q} = \left\{\frac{(1-n)}{K_s} + \frac{n}{K_w}\right\} \quad (1)$$

k_w is the permeability coefficient, p_w is the pore pressure, v_s is the velocity of soil skeleton, $\frac{D}{Dt}$ refers to a material derivative following the soil particles, and the equivalent volumetric stiffness, Q, is given in terms of soil porosity n, volumetric stiffness of pore water K_w and soil grains K_S.

(2) The balance of linear momentum for the mixture of soil skeleton–pore fluid is

$$\rho\frac{Dv_0}{Dt} = \rho b + div\,\sigma \quad (2)$$

ρ is the density of the mixture, b the body forces and σ the Cauchy stress tensor.

From here, it is possible to derive the propagation–consolidation model, writing the equations in non-dimensional form, as proposed by Hutter and Koch (1991), and assuming that both the velocity and the pore pressure fields can be split into two components: propagation and consolidation:

$$v = v_0 + v_1 \; p_w = p_{w0} + p_{w1} \quad (3)$$

In above, the sub-index '0' refers to the propagation and '1' to the consolidation.

Figure 1 illustrates the reference system and some magnitudes of interest which will be used in this section.

The equations of the propagation–consolidation model are:

$$\rho\frac{Dv_0}{Dt} = \rho b + div\,\sigma \quad (4)$$

$$div\,v_0 = 0 \quad (5)$$

$$\frac{Dp_w}{Dt} = \frac{\partial}{\partial x_3}\left(c_v\frac{\partial p_w}{\partial x_3}\right) \quad (6)$$

v_0 is the velocity field corresponding to propagation, c_v is the coefficient of consolidation.

From now on, we will drop the sub-index '1' for the sake of simplicity.

Equations (4–6) can be integrated along the depth, resulting in a 2D problem which is much simpler. Depth-integrated models have been frequently used in the past to model flow-like landslides. It is worth mentioning the work of Hutter Hutter and Koch (1991), Laigle and Coussot (1997), Pastor et al. (2002) and McDougall and Hungr (2004).

The balance of mass and momentum equations obtained in the preceding section can be integratedalong the depth (x_3) taking into account the Leibniz's rule.

The model consists of the following equations:

Balance of mass

$$\frac{\partial h}{\partial t} + \frac{\partial}{\partial x_j}(\bar{v}_j h) = e_R \qquad j = 1,\ 2 \quad (7)$$

$\bar{v}_j$ is the depth-averaged velocity along x_i and e_R is an erosion velocity parameter. Sub-indexes i and j refer to axes 1 and 2.

Balance of momentum

$$\frac{\partial}{\partial t}(h\bar{v}_i) + (1+\alpha)\frac{\partial}{\partial x_j}(h\bar{v}_i\bar{v}_j) = b_i h + \frac{1}{\rho}\frac{\partial}{\partial x_j}(h\bar{\sigma}_{ij}) + \frac{1}{\rho}\left|N^A\right|t_i^A + \frac{1}{\rho}\left|N^B\right|t_i^B \quad (8)$$

α is a correction factor which will depend on the velocity profile, t_i^A and $t_i^B$are the tractions acting on

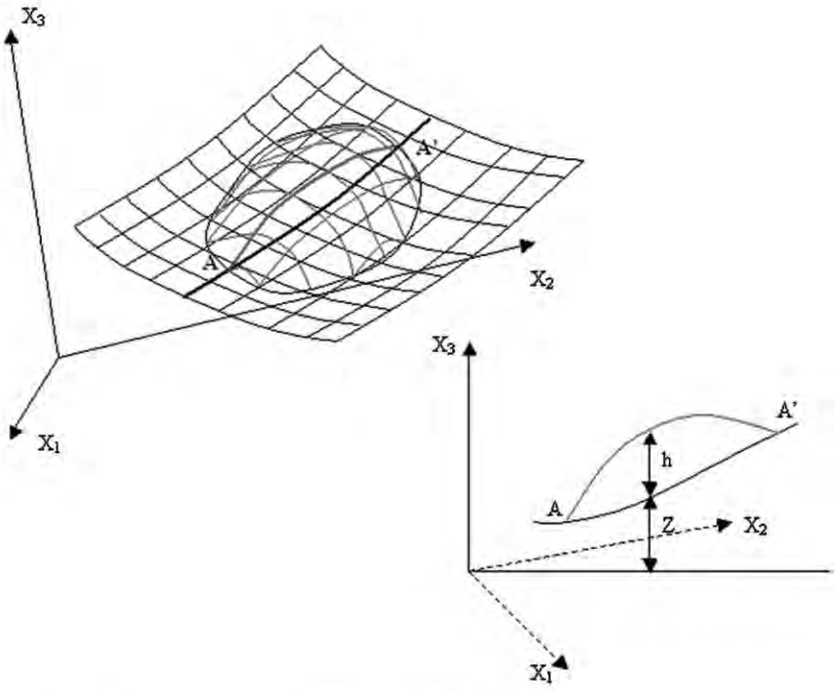

Figure 1. Reference system and the notations used in the analysis.

the surface and the bottom, respectively, $\bar{\sigma}_{ij}$ is the stress tensor averaged over depth, and N^A and N^B are two vectors normal to the surface and the bottom respectively, given by:

$$|N^B| = \left(\frac{\partial Z^2}{\partial x_1} + \frac{\partial Z^2}{\partial x_2} + 1\right)^{1/2}$$
$$|N^A| = \left(\left(\frac{\partial (Z+h)}{\partial x_1}\right)^2 + \left(\frac{\partial (Z+h)}{\partial x_2}\right)^2 + 1\right)^{1/2} \quad (9)$$

Concerning the vertical consolidation equation, it can be integrated along x_3 also, then:

$$\frac{\partial}{\partial t}(\bar{p}_w h) + \frac{\partial}{\partial x_j}(\bar{v}_j \bar{p}_w h) = c_v \left.\frac{\partial p_w}{\partial x_3}\right|_Z^{Z+h} \quad (10)$$

We will assume that pore pressure can be approximated by

$$p_w(x_1, x_2, x_3, t) = \sum_{k=1}^{Npw} P_k(x_1, x_2, t)\, N_k(x_3) \quad (11)$$

$N_k(x_3)$ are shape functions used to approximate the variation of pore pressure along x_3. We will choose harmonic functions satisfying boundary conditions. If we assume that pore pressure is zero at the surface and the bottom is impervious:

$$N_k(x_3) = \cos\frac{(2k-1)}{2h}\pi(x_3 - Z) \quad k = 1, N_{p_w} \quad (12)$$

Limiting the analysis to a single Fourier component, we obtain

$$\frac{\partial}{\partial t}(P_1 h) + \frac{\partial}{\partial x_j}(\bar{v}_j P_1 h) + \frac{\pi}{2} C.T. = -\frac{\pi^2}{4h} c_v P_1 \quad (13)$$

P_1 depends on x_1, x_2 and t, and $C.T.$ stands for 'correction terms' which we have neglected.

2.2. *An alternative quasi-Lagrangian formulation*

The approach described above is Eulerian, usually found in finite elements, differences and volumes formulations. As an alternative, meshless methods provide important advantages regarding conservation properties and computation times. Here, we present a depth-integrated quasi-Lagrangian formulation. The name comes from the fact that velocities are not constant over depth. Therefore, we are not considering a constant mass of the avalanching soil attached to a particular node. To derive this formulation of the depth-integrated equations, we introduce a 'quasi material derivative' as:

$$\frac{\bar{d}}{dt} = \frac{\partial}{\partial t} + \bar{v}_j \frac{\partial}{\partial x_j} \quad (14)$$

The resulting model consists of the following equations:

Balance of mass

$$\frac{\bar{d}h}{dt} + h\frac{\partial \bar{v}_j}{\partial x_j} = e_R \tag{15}$$

Balance of momentum

$$\begin{aligned} h\frac{\bar{d}}{dt}\bar{v}_i - \frac{\partial}{\partial x_i}\left(\frac{1}{2}b_3 h^2\right) \\ = -e_R\bar{v}_i - \alpha\frac{\partial}{\partial x_j}\left(h\bar{v}_i\bar{v}_j\right) + b_i h + \frac{1}{\rho}\frac{\partial}{\partial x_j}\left(h\bar{\sigma}^*_{ij}\right) + \frac{1}{\rho} \\ \times \left|N^A\right| t_i^A + \frac{1}{\rho}\left|N^B\right| t_i^B \end{aligned} \tag{16}$$

Consolidation

$$\frac{\bar{d}P_1}{dt} + \frac{1}{h}P_1 e_R + \frac{\pi}{2h}C.T. = -\frac{\pi^2}{4h^2}c_V P_1 \tag{17}$$

3. Rheological model

The depth-integrated model described in the preceding section includes terms which depend on the rheological properties of the fluidised soil: the basal friction and the depth-integrated stresses. It is important to note that they depend on the flow structure along the depth, which has been lost in the depth-integration procedure. In order to obtain these terms at a particular point, we assume that the depth-integrated velocity and height are those of an infinite landslide (a stationary landslide of infinite length where properties are only functions of depth).

There are many alternative rheological models which have been proposed in the past, of which we have used two in this work: the Bingham cohesive fluid and the frictional fluid, which we have enriched with the Voellmy's term.

3.1. Bingham fluid

In Bingham fluids, it is not possible to obtain directly the shear stress at the bottom as a function of the average velocity. The expression relating the average velocity to the basal friction for the infinite landslide problem is

$$\bar{\nu} = \frac{\tau_B h}{6\mu}\left(1 - \frac{\tau_Y}{\tau_B}\right)^2\left(2 + \frac{\tau_Y}{\tau_B}\right) \tag{18}$$

μ is the viscosity, τ_Y the yield stress and the shear stress on the bottom, τ_B, is given by:

$$\tau_B = \tau_Y\frac{h}{h_P} = \frac{\tau_Y}{\eta} \tag{19}$$

$\eta = h_p/h$ is the ratio between the height of the constant velocity region or plug to the total height of the flow.

We have introduced a non-dimensional number a defined as:

$$a = \frac{6\mu\bar{v}}{h\tau_Y} \tag{20}$$

Then, rearranging Equation (18):

$$\frac{\bar{v}6\mu}{\tau_Y h}\eta = (1-\eta)^2(2+\eta) \tag{21}$$

This expression can be transformed into:

$$P_3(\eta) = \eta^3 - (3+a)\eta + 2 = 0 \tag{22}$$

It is necessary to obtain the root of a third-order polynomial. To decrease the computational load, several simplified formulae have been proposed in the past. Pastor et al. (2004b) used a simple method based on obtaining the second-order polynomial, which is the best approximation in uniform distance of the third-order polynomial:

$$P_2(\eta) = \frac{3}{2}\eta^2 - \left(\frac{57}{16} + a\right)\eta + \frac{65}{32} \tag{23}$$

Knowing the non-dimensional number a, the root is obtained immediately.

Concerning depth-averaged stresses, we have assumed the following relations to hold:

$$\begin{aligned} \sigma_{11} = \sigma_{22} = \sigma_{33} = -p \\ \sigma_{13} = \sigma_{31} = \tau_y + \mu\left(\frac{\partial v_1}{\partial x_3}\right) \end{aligned} \tag{24}$$

3.2. Frictional fluid

One simple yet effective model is the frictional fluid, especially in the case where it is used within the framework of coupled behaviour between soil skeleton and pore fluid.

The frictional model is independent of the velocity, therefore without further additional data it is not possible to obtain the velocity distribution.

Concerning the basal friction, it is considered that the shear stresses are concentrated in a narrow band

very close to the bottom. The basal friction along x_i is:

$$\tau_b = -\sigma_v tan\phi \frac{\bar{v}_i}{|\bar{v}|} \tag{25}$$

σ_v is the normal stress acting on the bottom, $\bar{v}_i$ the depth-averaged velocity along the axis i, $|\bar{v}|$ the module of depth-averaged velocity and ϕ the friction angle of the fluidised soil.

This expression can be refined by taking into account the existence of pore pressures in the fluidised soil and the possibility of a smaller friction angle in the contact soil-basal material:

$$\tau_b = -\rho'_d gh tan\phi_b \frac{\bar{v}_i}{|\bar{v}|} \tag{26}$$

The basal friction ϕ_b is

$$\phi_b = min(\delta_k, \phi) \tag{27}$$

The effect of pore pressures is taken into account by:

$$\tau_b = -\left((\sigma_v - p_w^b)\tan\phi_b\right)\frac{\bar{v}_i}{|\bar{v}|} \tag{28}$$

Sometimes, when there is a high mobility of granular particles and drag forces due to the contact with the air are important, it is convenient to introduce the extra-term proposed by Voellmy, $\frac{\rho g v^2}{\xi}$, where ξ is the turbulence parameter.

$$\tau_b = -\left\{\left(\rho'_d gh\ tan\phi_b - p_w^b\right)\frac{\bar{v}_i}{|\bar{v}|} + \rho g \frac{|\bar{v}|}{\xi}\bar{v}_i\right\} \tag{29}$$

4. Numerical model

To analyse the propagation of a fast landslide over a terrain, there are two main alternatives. The first is Eulerian, and is based on a structured (finite differences) or unstructured grid (finite elements and volumes) within which the material flows. The main

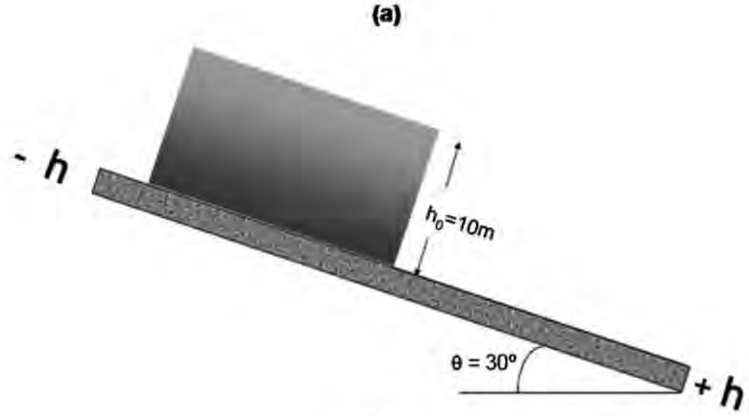

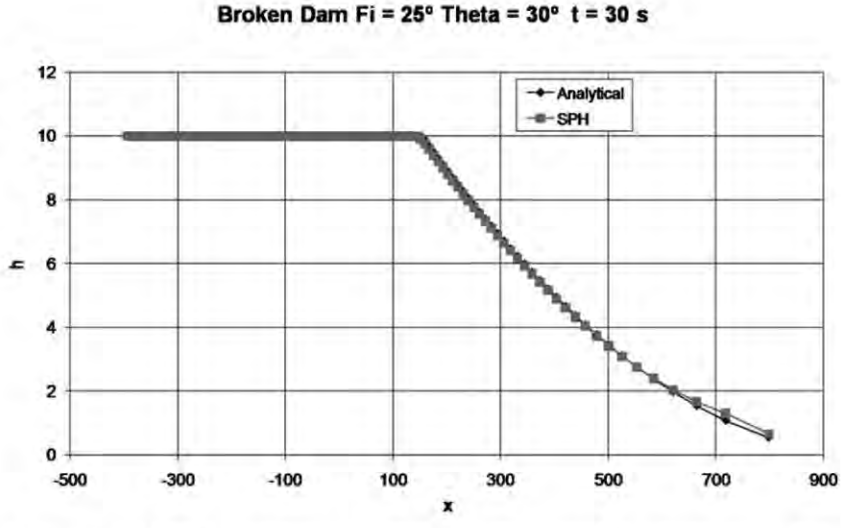

Figure 2. Dam break problem. (a) Initial conditions. (b) Analytical vs. computed solution at $t = 30$ s.

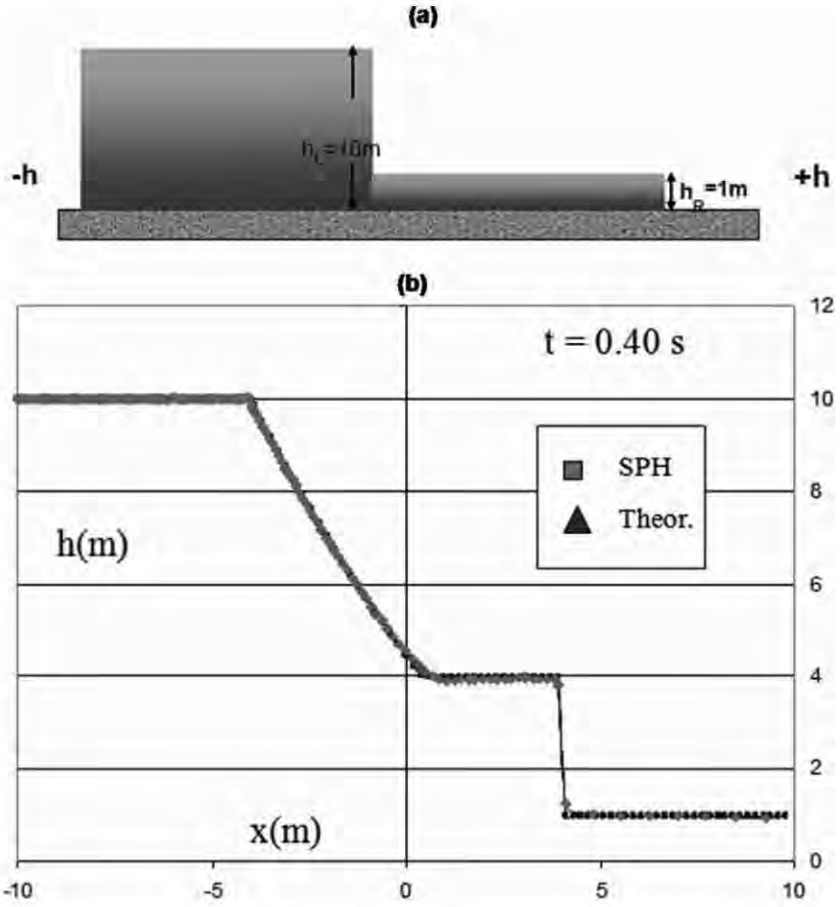

Figure 3. Dam break over a wet surface. (a) Initial conditions. (b) Analytical vs. computed solution at $t = 0$, 4 s.

problem here is the need of a very fine computational mesh for both the terrain information and for the fluidised soil. The second, Lagrangian methods, allow the separation of both meshes, with an important economy of computational effort. If we combine a Lagrangian method with a mesh-based discretisation technique, we will find problems as soon as the mesh deforms, making it necessary to use mesh refinement. In this work we have used a different and interesting alternative, a meshless method, referred to as SPH.

SPH is a meshless method introduced independently by Lucy (1977) and Gingold and Monaghan (1977) and firstly applied to an astrophysical modelling, a domain where SPH presents important advantages over other methods. SPH is well suited for hydrodynamics, and researchers have applied it to a variety of problems, like those described in Gingold and Monaghan (1982), Monaghan and Gingold (1983), Monaghan et al. (1999), Monaghan, Kos, and Issa (2003) and Bonet and Kulasegaram (2000). SPH has also been applied to model the propagation of catastrophic landslides (McDougall and Hungr 2004; Bonet and Rodríguez 2005). However, in both cases, the analysis did not incorporate the hydro-mechanical coupling between the solid skeleton and the pore fluid, which has been proposed by Pastor et al. (2009).

4.1. An SPH method for depth-integrated equations

It is possible to obtain SPH model for the depth-integrated Equations (15–17), the result being a set of ordinary differential equations (ODEs).

First, we will introduce a set of nodes $\{x_K\}$ with $K = 1 \ldots N$, and the following nodal variables: h_I, height of the landslide at node I; $\bar{v}_I$, depth-averaged, 2D velocity; t_I^b, surface force vector at the bottom; $\bar{\sigma}_I^*$, depth-averaged modified stress tensor; P_{1I}, pore pressure at the basal surface; e_R, erosion velocity parameter.

Then, we considered Ω_I as the 2D area associated to node I, and we introduced the following terms:

(1) a fictitious mass m_I moving with this node:

$$m_I = \Omega_I h_I \tag{30}$$

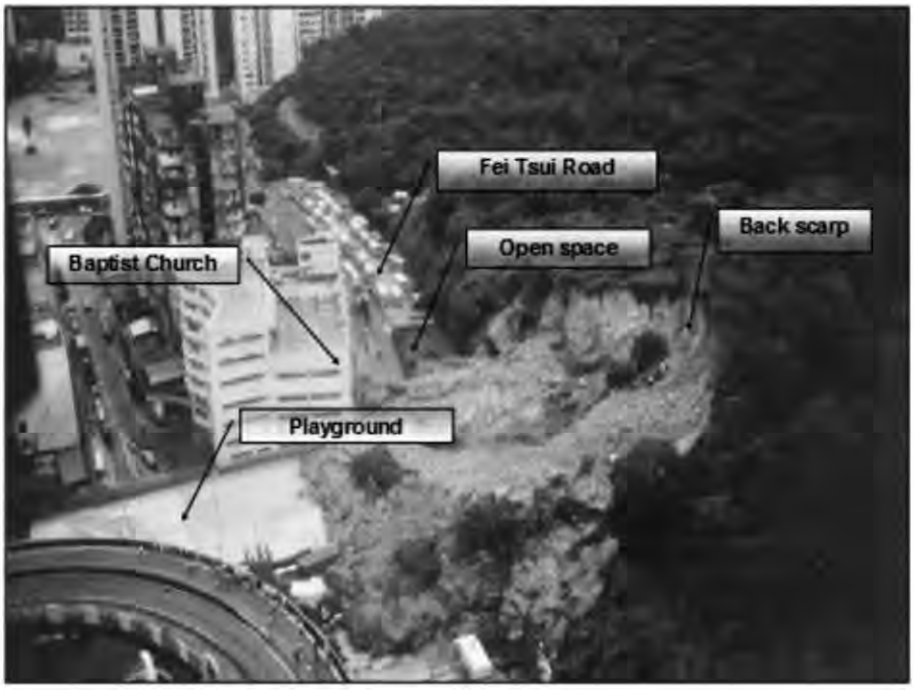

Figure 4. General view of Fei Tsui Road landslide (Knill and GEO 2006b).

(2) an averaged pressure term $\bar{p}_I$, given by:

$$\bar{p}_I = \frac{1}{2} b_3 h_I^2 \tag{31}$$

b_3 is the component of body forces (gravity) along x_3 axis.

It is important to note that m_I has no physical meaning, since when node I moves, the material contained in a column of base Ω_I has entered it or will leave it as the column moves with an averaged velocity which is not the same for all particles in it.

There are several possible alternatives for the equations, according to the discretised form chosen for the differential operator results. Concerning the continuity of mass equations, there are two alternatives; the former consists of the equation:

$$\frac{\bar{d}h_I}{dt} = e_R + h_I \sum_J \frac{m_J}{h_J} v_{IJ}\, grad\, W_{IJ} \tag{32}$$

where, W_{IJ} is the weighting function classical of SPH methods, and we have introduced $v_{IJ} = v_I - v_J$.

Alternatively, the height can be obtained once the position of the nodes is known:

$$h_I = \langle h(x_I) \rangle = \sum_J h_J \Omega_J W_{IJ} = \sum_J m_J W_{IJ} \tag{33}$$

The discretised balance of linear momentum equation is:

$$\frac{\bar{d}}{dt}\bar{v}_I = -\sum_J m_J \frac{p_I + p_J}{h_I h_J} grad\, W_{IJ} + \frac{1}{\rho} \times \sum_J m_J \frac{\sigma_I + \sigma_J}{h_I h_J} grad\, W_{IJ} + b + \frac{1}{\rho h_I} \left| N^B \right| t_I^B - \frac{1}{h_I} e_R \bar{v} \tag{34}$$

Finally, the SPH discretised form of the basal pore pressure dissipation is:

$$\frac{\bar{d}}{dt} P_{1I} = -\frac{\pi^2 c_v}{4 h_I} P_{1I} \tag{35}$$

So far, we have discretised the equations of balance of mass, balance of momentum and pore pressure dissipation. The resulting equations are Ordinary Differential Equations (ODEs), which have been integrated in time using a scheme Runge Kutta fourth order.

Table 1. Parameters used to model Fei Tsui landslide.

Fei Tsui Landslide	
Density	19 KN/m^3
Erosion factor	No erosion
Drainage condition	Undrained behaviour
Rheological model	Frictional fluid
Friction angle (apparent)	26°

5. Model application

5.1. General remarks

This section presents some of the results obtained by employing the SPH model. First, we present a validation of the model using two cases for which there are analytical solutions: (1) dam break of a frictional fluid over an inclined plane and (2) dam break over a wet horizontal plane.

Then, we consider two real cases of short runout landslides which occurred in Honk Kong on 13 August 1995 in the wake of typhoon Helen: Fei Tsui and Shum Wan Landslides. In those events, the material had basically moved to the bottom of the slope without travelling a significant distance from its source. In order to reproduce accurately the most important features of the phenomena such as travel trajectory,

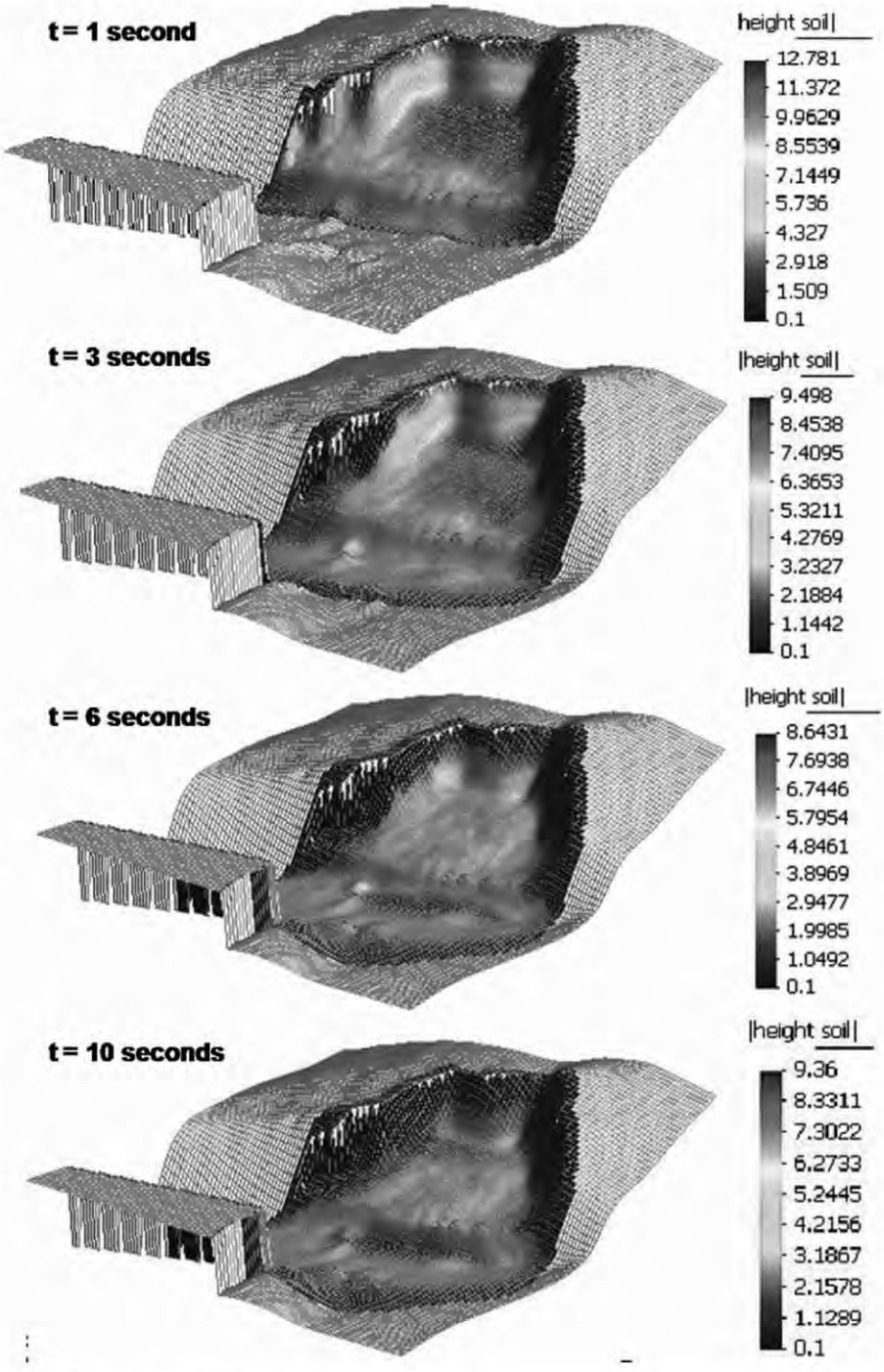

Figure 5. Propagation of Fei Tsui landslide.

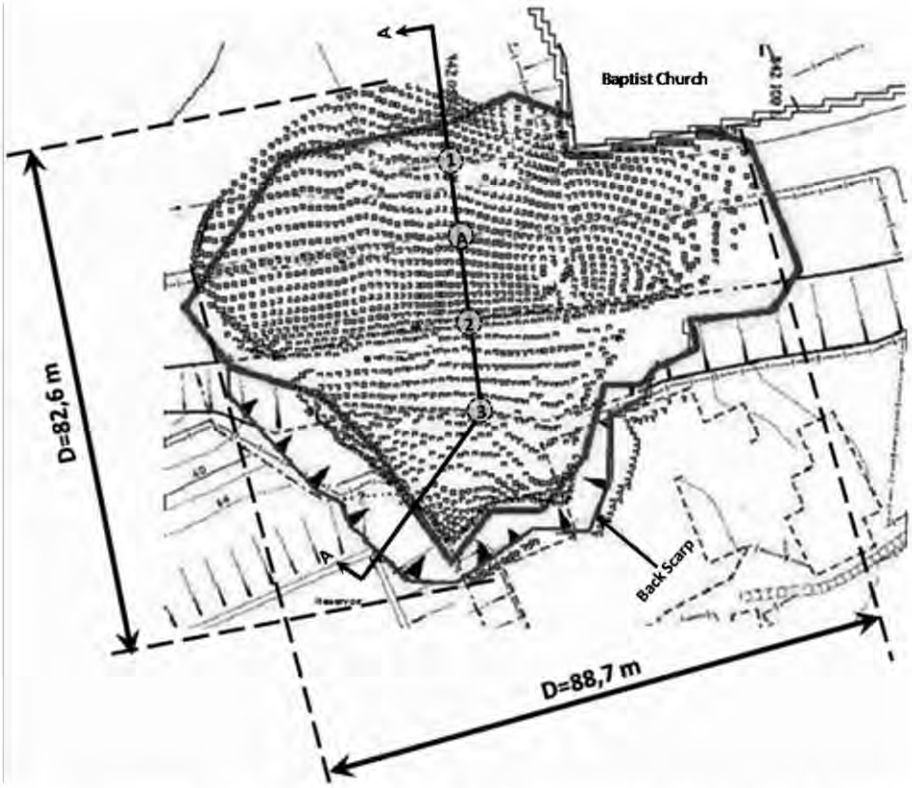

Figure 6. Comparison for the extent of the landslide between field measurements and computed results.

runout distance, total area and depth of final deposits, a trial and error calibration procedure were used.

5.2. Dam break of a frictional fluid on an inclined plane

The dam break problem has been used in the past to assess the performance of proposed models. The case we model here has a solution as proposed by Mangeney et al. (2000). The analytical solution is given by:

$$h(t) = \begin{cases} h_0 & x \le x_L \\ \frac{1}{9g\cos\theta}\left(2c_0 - \frac{x}{t} - \frac{1}{2}mt\right)^2 & x_L \le x \le x_R \\ 0 & x_R \le x \end{cases} \quad (36)$$

The coordinate system used here is an x axis along the inclined plane and h being measured along its normal. x_L and x_R represent the limits of the expansion wave, which can be obtained by making $h(t) = h_0$ and $h(t) = 0$, respectively, in Equation (36).

Figure 2(a) illustrates initial conditions: initial depth ($h_0 = 10$ m), bed inclination ($\kappa = 30^\circ$) and friction angle ($\phi = 25^\circ$).

This test case provides information on how the model deals with source terms originated by the sloping terrain and the friction. The results obtained at 30 s showed a good agreement between the theoretical and the computed results (Figure 2(b)).

5.3. Dam break of a frictional fluid on wet bed

Dam breaking over a wet horizontal plane is more suitable for measuring the ability of the model to reproduce shock waves.

The case under analysis consists of a dam located at the origin, and the surface of water has two zones: on the left, the 10-m high dam which extends to $-\infty$, and on the right, a bed flooded with water 1-m deep (Figure 3(a)). Analytical and computed wave profiles at $t = 0$, 4 s are provided in Figure 3(b). The solution consists of:

(1) A rarefaction wave travelling to the left (see in the figure the transition from 10 m to a point close to $x = 1$ m, where depth is 4 m.
(2) A shock wave moving to the right, which is the water body of 4-m depth. The front is located at $x = 4$ m approximately.

The model predictions agree well with the analytical solution, and are free of oscillations or other spurious phenomena.

5.4. Fei Tsui Road landslide

This landslide, described in Knill and Geotechnical Engineering Office (2006b), occurred in a slope of

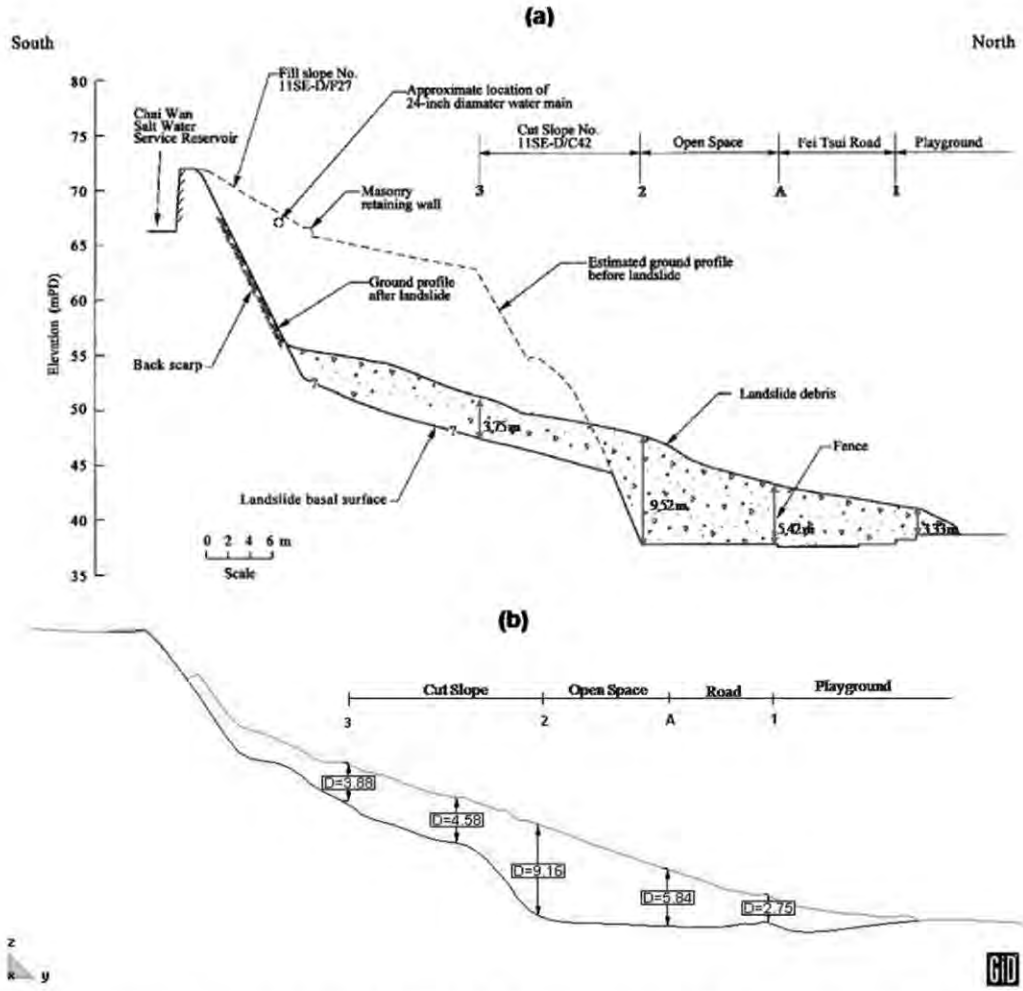

Figure 7. Comparison between vertical profiles A–A′: (a) Field measurements. (b) Computed results.

weathered volcanic rock, from moderately to completely weathered tuff, involved 14,000 m^3 of material. The movement was caused by a combination of a weaker material together with an increase in groundwater pressure following a long heavy rainfall. The slope was 60°, and densely vegetated. The mobilised mass was up to 90-m wide, and travelled about 70 m. The landslide piled up against a corner of the building (Baptist Church) some 6-m deep. Figure 4 shows a general view of the landslide.

The landslide has been modelled using a frictional fluid, taking into account the propagation time (10 s) and the soil mass involved, and we have assumed an undrained behaviour (propagation time is significatively shorter than the time for pore pressure dissipation). Table 1 summarises the parameters used.

Figure 5 depicts the position of the landslide at times 1, 3, 6 and 10 s. Figure 6 includes the extension of final debris deposition, both real and modelled. Figure 7(a) and (b) shows the same vertical profile A–A′, with site measurements and model predictions at specific points, respectively.

We have evaluated the precision of the results by comparing the values in the model with field measurements. As references, we have chosen the runout, the dimensions of the debris deposit and the thickness of the material deposited at some points of the profile A–A′, and the corner of the church (point P).

The agreement for the depth and the maximum width of the deposit was excellent, and the result for the runout was good enough. However, the maximum distance travelled was overestimated by 18%. Table 2 contains the actual values, the programme's results and the differences expressed as percentages.

5.5. *Shum Wan Landslide*

The Shum Wan landslide occurred on a natural hillside between the roads of Shum Wan and Nam Long, sloped at about 27° and densely vegetated. It was

Table 2. Values for the actual debris deposits and model.

	Landslide (m)	Modelling (m)	Difference (%)
Maximum width of the debris deposit	90	88.70	−1.44
Maximum horizontal distance	70	82.60	+18.00
Depth on point 2, profile A–A′	9.52	9.16	−3.78
Depth on point 3, profile A–A′	3.75	3.88	+3.47
Depth on point A, profile A–A′	5.42	5.84	+7.75
Depth on point 1, profile A–A′	3.33	2.75	−17.41
Maximum depth of debris piled against the corner of the church (point P)	6	5.20	+13.3

triggered by an exceptional rainfall and favoured by the discharge of water collected along the latter road. The slope failed, taking away Nam Long Shan Road. The debris flowed across Shum Wan Road, reaching some 70 m from the toe of the slope. The slide scar was about 140 m long, 50 m wide at the level of Nam Long Shan and 90 m wide above Shum Wan Road.

The landslide involved some 26,000 m^3 of weathered ash and tuff. A thick clay seam controlled the failure surface. Figure 8 shows a general view of the landslide.

The analysis has been performed on the basis of the information available from Knill and GEO (2006a), and the digital terrain models provided by Hong Kong Geotechnical Engineering Office.

Rheological behaviour in that medium length movement is difficult to specify *a priori*, due to the combination of effects that modified the initial frictional conditions. The case was modelled several times, combining the following conditions and characteristics: rheology (frictional, Voellmy or Bingham), drainage conditions (undrained behaviour or partial dissipation of pore water pressure) and variability of material strength along the path (one or several material). Table 3 summarises the parameters used in each case.

After a number of trials were determined matching the various trial runs with the observed distribution of debris deposit, we found that the best fit was produced using the Bingham model, because it represents, with reasonable accuracy, the area and the small thickness of the deposited material that spreads at the end. The fit for path length was slightly better using Frictional and Voellmy models, but they failed in capturing the entire behaviour of the flow.

The reason for this difference is probably that Bingham model is better in considering the clayey composition of the material and the important water discharge in the later stages of the debris flow. Also, the Bingham model is consistent with the significant plasticity of the material forming the base of the slide. Similar results were found by Geertsema et al. (2006) at Pink Mountain, Canada, concluding that a small

Figure 8. General view of Shum Wan Landslide (Knill and GEO 2006a).

Table 3. Parameters used to model Shum Wan Landslide.

Shum Wan Landslide		
Density	19 KN/m^3	
Erosion factor	No erosion	
Rheological model	Frictional fluid	
Drainage condition	Undrained behaviour	Partial dissipation of pore pressures $B_{fact} = 1 \times 10^{-4}$ h_pwp_rel = 0.27 pwp_rel = 0.007
Number of zones with different materials along the path	4	4
Friction angle of materials along the path (Basal friction angle) (°)	Zone 1: $\phi_b = 33$ Zone 2: $\phi_b = 21$ Zone 3: $\phi_b = 16$ Zone 4: $\phi_b = 32$	Zone 1: $\phi_b = 39$ Zone 2: $\phi_b = 26$ Zone 3: $\phi_b = 21$ Zone 4: $\phi_b = 38$
Internal friction angle (°)	25.5	24
Rheological model	Voellmy frictional fluid	
Drainage condition	Undrained	Partial dissipation of pore pressures $B_{fact} = 1 \times 10^{-4}$ h_pwp_rel = 0.27 pwp_rel = 0.007
Number of zones with different materials along the path	4	4
Friction angle of materials along the path (Basal friction angle) (°)	Zone 1: $\phi_b = 33$ Zone 2: $\phi_b = 21$ Zone 3: $\phi_b = 16$ Zone 4: $\phi_b = 32$	Zone 1: $\phi_b = 39$ Zone 2: $\phi_b = 26$ Zone 3: $\phi_b = 21$ Zone 4: $\phi_b = 38$
Internal friction angle (°)	15	20
Turbulence coefficient (m/s^2)	400	400
Rheological model	Bingham fluid	
Drainage condition	Undrained	
Viscosity (Pa s)	500	
Yield strength (Pa)	15,000	

Notes: B_{fact} = coefficient of basal pressure dissipation ($B_{fact} = \frac{\pi^2 c_v}{4}$).
h_pwp_rel = relative width of basal saturated layer to the total depth (dimensionless, vary between 0.25 and 1).
pwp_rel = maximum excess pore water pressure at the basal surface (dimensionless, vary between 0 and 1, last value correspond to liquefaction).

rock avalanche mobilising and entraining large quantities of plastic clayey material could only be modelled realistically using the Bingham model, in order to duplicate a thin, even spreading of the deposit.

The Bingham properties are: yield shear strength of 15,000 Pa and a viscosity of 500 Pa s. Debris motion ceased after 25 s.

Figure 9 displays the simulated depth contour distributions of debris at 0, 5, 10, 15, 20 and 25 s. Figure 10 includes both extension and depth values estimated and the comparison with actual values. The final profiles (section A–A′) measured on site and calculated are shown in Figure 11(a) and (b), respectively.

The final deposition of debris estimated using SPH agrees well with the site observation. The estimated and actual runout are very similar, and the results for the width and distance travelled are very close to real measurements. Nevertheless, there is an over-predicted lateral spreading towards the left side. As for the deposit depth evaluated in the section A–A, the adjustment is good enough.

6. Conclusions

Depth-integrated models have been applied to many cases of flow slides and debris flows where the propagation distance is large. However, in the case of landslides with much shorter propagation distances (of the same order than their length) not many cases have been published.

The proposed method presents limitations inherent to the assumptions made. In our opinion, the main limitation is not running with the same model in

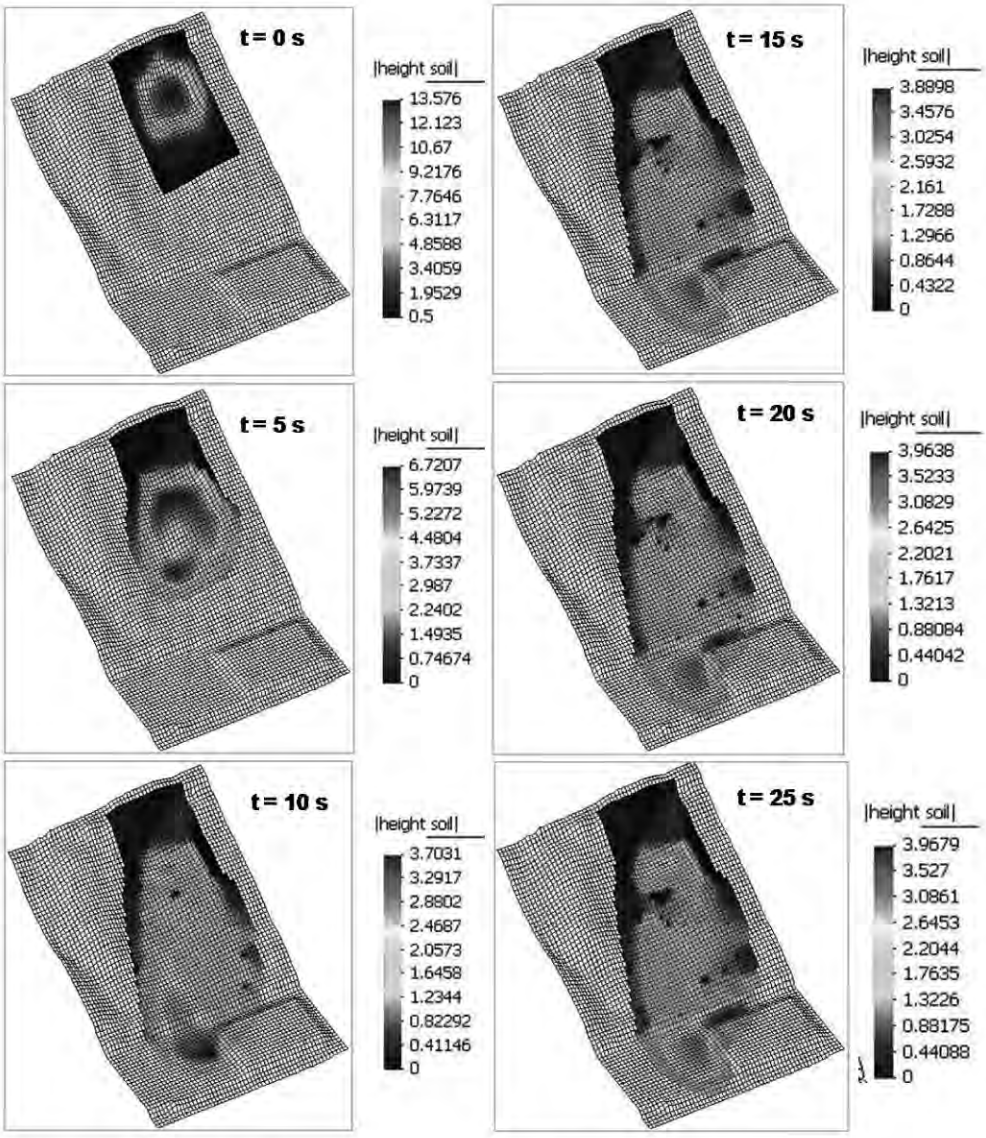

Figure 9. Calculated sequences for select times. Flooded contours show the corresponding depth.

both triggering and propagation phases. In general, the main difficulty comes from using different material models, in the case of triggering a constitutive equation and in propagation a rheological model. A possible bridge could be using Perzyna's viscoplasticity. In addition to this, evolution of pore pressure has to be dealt with more precision. Just one simple shape function (a quarter of a cosinus) is not enough, and more enriched functions (even a finite difference mesh along the depth) could provide a better approximation.

The main uncertainty is the determination of the parameters of the rheological model. Using laboratory rheometers can be a solution, provided the size of particles is very small. Otherwise, back analysis of similar cases has to be used.

Concerning sensitivity, the interested reader will find in Haddad et al. (2010) information in the case of lahars.

The main advantage of depth-integrated models is their simplicity. Complex cases run in standard personal computers in less than 5 min. Choosing finite elements, volumes or SPH is a matter of which code is available to the analyst. SPH is, in our opinion, faster.

This paper has presented: (1) a depth-integrated SPH model, which, once validated, can be applied to model landslide propagation and (2) two applications to real cases which occurred in Hong Kong in August 1995, for which there is relevant information available.

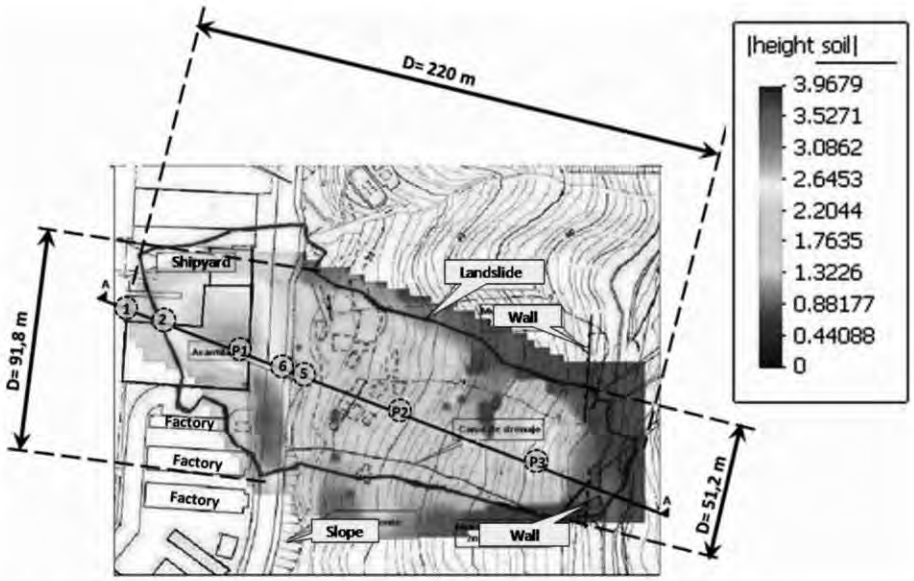

Figure 10. Calculated deposition of depth distribution, and contour of real landslide.

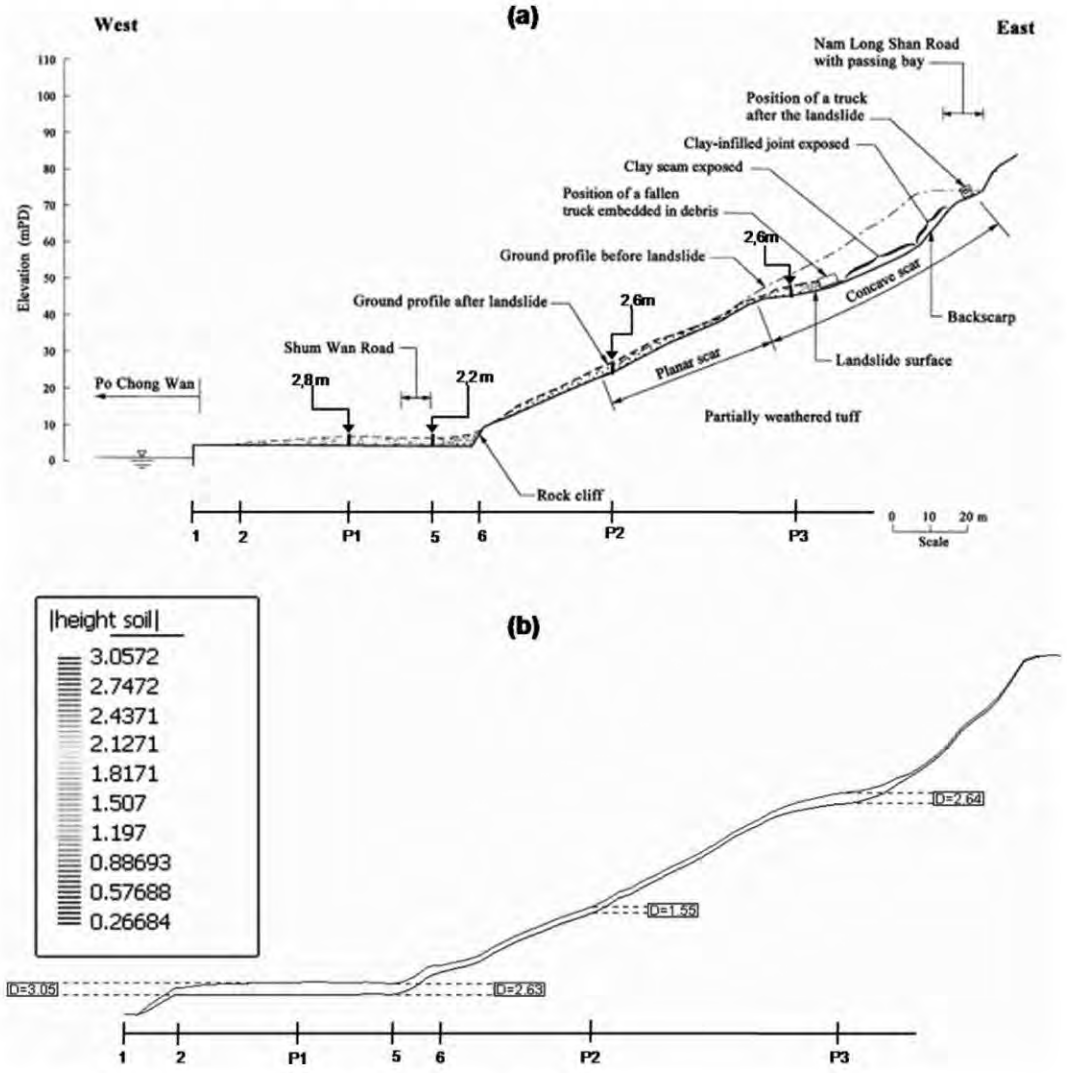

Figure 11. Profiles: (a) Field measurements. (b) Calculated.

The computed results show good agreement with the observations, and therefore, the proposed method can be applied in other cases.

Acknowledgements

The authors gratefully acknowledge the permission granted by the Hong Kong Geotechnical Office for publishing the results of Section 5. We also thank the European Union (Project Safeland) and the former Spanish MCINN (Project Geodyn).

References

Biot, M. A. 1941. "General Theory of Three-dimensional Consolidation." *Journal of Applied Physics* 12 (2): 155–164. doi:10.1063/1.1712886

Biot, M. A. 1955. "Theory of Elasticity and Consolidation for a Porous Anisotropic Solid." *Journal of Applied Physics* 26 (2): 182–185. doi:10.1063/1.1721956

Bonet, J., and S. Kulasegaram. 2000. "Correction and Stabilization of Smooth Particle Hydrodynamics Methods with Applications in Metal Forming Simulations." *International Journal for Numerical Methods in Engineering* 47 (6): 1189–1214. doi:10.1002/(SICI)1097-0207(20000228)47:6<1189::AID-NME830>3.0.CO;2-I

Bonet, J., and M. X. Rodríguez Paz. 2005. "A Corrected Smooth Particle Hydrodynamics Formulation of the Shallow-water Equations." *Computers and Structures* 83 (17–18): 1396–1410. doi:10.1016/j.compstruc.2004.11.025

Coulomb, C. A. 1773. "Essai sur une application des règles de Maximis & Minimis à quelques Problèmes de statique relatifs à l'Architécture [Test on the Rules of Maximus and Minimus a Few Problems Reated to the Static Architecture]." *Mémoires de Mathématique et de Physique Présentés à l' Académie Royale des Sciences, par divers sçavans, & lûs dans ses assemblées* [Memoirs of Mathematics and Physics presented at the Royal Academy of Sciences, by Various Learned Men, and Read in his Meetings] 7: 343–382.

Coussy, O. 1995. *Mechanics of Porous Media*. Chichester: Wiley.

D'Ambrosio, D., Iovine G., Spataro W., and Miyamoto H. 2007. "A Macroscopic Collisional Model for Debris-flows Simulation." *Environmental Modelling & Software* 22 (10): 1417–1436. doi:10.1016/j.envsoft.2006.09.009

De Boer, R. 2000. *Theory of Porous Media*. Berlin: Springer. doi:10.1007/978-3-642-59637-7.

Geertsema, M., O. Hungr, J. W. Schwab, and S. G. Evans. 2006. "A Large Rockslide–Debris Avalanche in Cohesive Soil at Pink Mountain, Northeastern Bristish Columbia, Canada." *Engineering Geology* 83 (1–3): 64–75. doi:10.1016/j.enggeo.2005.06.025

Gingold, R. A., and J. J. Monaghan. 1977. "Smoothed Particles Hydrodynamics: Theory and Application to Non-spherical Stars." *Monthly Notices of the Royal Astronomical Society* 181: 375–389.

Gingold, R. A., and J. J. Monaghan. 1982. "Kernel Estimates as a Basis for General Particle Methods in Hydrodynamics." *Journal of Computational Physics* 46 (3): 429–453. doi:10.1016/0021-9991(82)90025-0

Haddad, B., M. Pastor, D. Palacios, and E. Muñoz-Salinas. 2010. "A SPH Depth Integrated Model for Popocatépetl 2001 Lahar (Mexico): Sensitivity Analysis and Runout Simulation." *Engineering Geology* 114 (3–4): 312–329. doi:10.1016/j.enggeo.2010.05.009

Hutchinson, J. N. 1986. "A Sliding–Consolidation Model for Flow Slides." *Canadian Geotechnical Journal* 23 (2): 115–126. doi:10.1139/t86-021

Hutter, K., and T. Koch. 1991. "Motion of a Granular Avalanche in an Exponentially Curved Chute: Experiments and Theoretical Predictions." *Philosophical Transactions of the Royal Society of London, A* 334: 93–138. doi:10.1098/rsta.1991.0004

Iovine, G., and Mangraviti P. 2009. "The CA-model FLOW-S* for Flow-type Landslides: An Introductory Account." In *Proceedings of the 18th World IMACS Congress and MODSIM09*. Modelling and Simulation Society of Australia and New Zealand and International Association for Mathematics and Computers in Simulation, 2679–2685.

Iverson, R. I., and R. P. Denlinger. 2001. "Flow of Variably Fluidized Granular Masses across Three-Dimensional Terrain: 1. Coulomb Mixture Theory." *Journal of Geophysical Research* 106 (B1): 537–552. doi:10.1029/2000JB900329

Knill, S. J., and Geotechnical Engineering Office. 2006a. *Report on the Shum Wan road landslide of 13 august 1995. GEO REPORT 178*. Geotechnical Engineering Office, Civil Engineering and Development Department, Government of the Hong Kong Special Administrative Region.

Knill, S. J., and Geotechnical Engineering Office. 2006b. *Report on the Fei Tsui road landslide of 13 august 1995. GEO REPORT 188*. Geotechnical Engineering Office, Civil Engineering and Development Department, Government of the Hong Kong Special Administrative Region.

Laigle, D., and P. Coussot. 1997. "Numerical Modelling of Mudflows." *Journal of Hydraulic Engineering* (ASCE) 123 (7): 617–623. doi:10.1061/(ASCE)0733-9429(1997)123:7(617)

Lewis, R. L., and B. A. Schrefler. 1998. *The Finite Element Method in the Static and Dynamic Deformation and Consolidation of Porous Media*. New York: Wiley.

Lucy, L. B. 1977. "A Numerical Approach to the Testing of the Fission Hypothesis." *The Astronomical Journal* 82: 1013–1024. doi:10.1086/112164

Mangeney, A., P. Heinrich, and R. Roche. 2000. "Analytical Solution for Testing Debris Avalanche Numerical Models." *Pure and Applied Geophysics* 157 (6–8): 1081–1096. doi:10.1007/s000240050018

McDougall, S., and O. Hungr. 2004. "Model for the Analysis of Rapid Landslide Motion across Three-Dimensional Terrain." *Canadian Geotechnical Journal* 41 (6): 1084–1097. doi:10.1139/t04-052

Monaghan, J. J., R. A. F. Cas, A. M. Kos, and M. Hallworth. 1999. "Gravity Currents Descending a Ramp in a Stratified Tank." *Journal of Fluid Mechanics* 379: 39–69. doi:10.1017/S0022112098003280

Monaghan, J. J., and R. A. Gingold. 1983. "Shock Simulation by the Particle Method SPH." *Journal of Computational Physics* 52 (2): 374–389. doi:10.1016/0021-9991(83)90036-0

Monaghan, J. J., A. Kos, and N. Issa. 2003. "Fluid Motion Generated by Impact." *Journal of Waterway, Port, Coastal, and Ocean Engineering* (ASCE) 129 (6): 250–259. doi:10.1061/(ASCE)0733-950X(2003)129:6(250)

Monaghan, J. J., and J. C. Lattanzio. 1985. "A Refined Particle Method for Astrophysical Problems." *Astronomy and Astrophysics* 149: 135–143.

Pastor, M., M. Quecedo, J. A. Fernández Merodo, M. I. Herreros, E. González, and P. Mira. 2002. "Modelling Tailing Dams and Mine Waste Dumps Failures." *Geotechnique* 52 (8): 579–591. doi:10.1680/geot.2002.52.8.579

Pastor, M., M. Quecedo, E. González, M. I. Herreros, J. A. Fernández Merodo, and P. Mira. 2004a. "Modelling of Landslides (II) Propagation." In *Degradation and Instabilities in Geomaterials*, edited by F. Darve and I. Vardoulakis, 319–367. New York: Springer, Wien.

Pastor, M., M. Quecedo, E. Gonzalez, M. I. Herreros, J. A. Fernandez Merodo, and P. Mira. 2004b. "Simple Approximation to Bottom Friction for Bingham Fluid Depth Integrated Models." *Journal of Hydraulic Engineering* (ASCE) 130 (2): 149–155. doi:10.1061/(ASCE)0733-9429(2004)130:2(149)

Pastor, M., B. Haddad, G. Sorbino, S. Cuomo, and V. Drempetic. 2009. "A Depth-Integrated, Coupled SPH Model for Flow-like Landslides and Related Phenomena." *International Journal for Numerical and Analytical Methods in Geomechanics* 33 (2): 143–172. doi:10.1002/nag.705

Pastor, M., D. Manzanal, J. A. Fernández Merodo, P. Mira, T. Blanc, V. Drempetic, M. J. Pastor, B. Haddad, and M. Sanchez. 2010. "From Solids to Fluidized Soils: Diffuse Failure Mechanisms in Geostructures with Applications to Fast Catastrophic Landslides." *Granular Matter* 132: 211–228. doi:10.1007/s10035-009-0152-4

Poisel, R., and A. Preh. 2004. "Run Out Models of Rock Slope Failures." *Felsbau* 22 (2): 46–50.

Quecedo, M., M. Pastor, M. I. Herreros, and J. A. Fernández Merodo. 2004. "Numerical Modelling of the Propagation of Fast Landslides using the Finite Element Method." *International Journal for Numerical Methods in Engineering* 59 (6): 755–794. doi:10.1002/nme.841

Savage, S. B., and K. Hutter. 1991. "The Dynamics of Avalanches of Granular Materials from Initiation to Runout. Part I: Analysis." *Acta Mechanica* 86 (1–4): 201–223. doi:10.1007/BF01175958

Zienkiewicz, O. C., A. H. C. Chan, M. Pastor, D. K. Paul, and T. Shiomi. 1990a. "Static and Dynamic Behaviour of Soils: A Rational Approach to Quantitative Solutions. I. Fully Saturated Problems." *Proceedings of the Royal Society of London, Series A* 429 (1877): 285–309. doi:10.1098/rspa.1990.0061.

Zienkiewicz, O. C., A. H. C. Chan, M. Pastor, B. A. Shrefler, and T. Shiomi. 1999. *Computational Geomechanics*. New York: Wiley.

Zienkiewicz, O. C., C. T. Chang, and P. Bettess. 1980. "Drained, Undrained, Consolidating Dynamic Behaviour Assumptions in Soils." *Geotechnique* 30 (4): 385–395. doi:10.1680/geot.1980.30.4.385

Zienkiewicz, O. C., and T. Shiomi. 1984. "Dynamic Behaviour of Saturated Porous Media: The Generalised Biot Formulation and Its Numerical Solution." *International Journal for Numerical and Analytical Methods in Geomechanics* 8 (1): 71–96. doi:10.1002/nag.1610080106

Zienkiewicz, O. C., and R. L. Taylor. 2000. *The Finite Element Method*. Vol. 2; 5th ed. Oxford: Butterworth and Heinemann.

Zienkiewicz, O. C., Y. M. Xie, B. A. Schrefler, A. Ledesma, and N. Bicanic. 1990b. "Static and Dynamic Behaviour of Soils: A Rational Approach to Quantitative Solutions. II. Semi-Saturated Problems." *Proceedings of the Royal Society of London, SA* 429 (1877): 311–321. doi:10.1098/rspa.1990.0062